applied sciences

MDPI

Article

Experimental Study on the Condensation Heat Transfer on a Wettability-Interval Grooved Surface

Shaojun Ren, Shangwen Gao, Ze Xu, Suchen Wu * and Zilong Deng

Key Laboratory of Energy Thermal Conversion and Control of Ministry of Education, School of Energy and Environment, Southeast University, Nanjing 210096, China
* Correspondence: suchenwu@seu.edu.cn

Abstract: To provide further insight into humid air condensation on hybrid surfaces, an experiment was conducted to visually investigate the condensation process on wettability-interval grooved surfaces, which had hydrophobic ridges and hydrophilic grooves. The droplet dynamic behavior and heat transfer performance of condensation on a wettability-interval grooved surface were explored and compared with four other functional surfaces, including the plain hydrophilic surface, plain hydrophobic surface, hydrophilic grooved surface, and hydrophobic grooved surface. The presence of hydrophobic ridges perpendicular to the groove direction and hydrophilic grooves allowed for the exclusion and easy spreading of droplets, respectively. Compared with the other four functional surfaces, the coupling phenomena during condensation, i.e., the spontaneous suction and directional drainage via hydrophilic grooves, were only found on the wettability-interval grooved surface. These could not only remove condensate quickly but also suppress the formation of the flooded liquid film, which was beneficial to the enhancement of heat transfer performance. It was proven by the experimental results that at subcooling 12 K, the condensation heat flux on the wettability-interval grooved surface reached 1280 W/m^2, which was 1.25 times that of the plain hydrophobic surface (1030 W/m^2), and 15% higher than that of the hydrophobic grooved surface (1110 W/m^2). This indicated that the wettability-interval microgrooves could effectively enhance humid air condensation heat transfer performance.

Keywords: condensation; wettability; microgrooves; spontaneous suction; directional drainage

check for updates

Citation: Ren, S.; Gao, S.; Xu, Z.; Wu, S.; Deng, Z. Experimental Study on the Condensation Heat Transfer on a Wettability-Interval Grooved Surface. *Appl. Sci.* **2023**, *13*, 10518. https://doi.org/10.3390/app131810518

Academic Editor: Weihua Cai

Received: 28 August 2023
Revised: 15 September 2023
Accepted: 19 September 2023
Published: 21 September 2023

Copyright: © 2023 by the authors. Licensee MDPI, Basel, Switzerland. This article is an open access article distributed under the terms and conditions of the Creative Commons Attribution (CC BY) license (https://creativecommons.org/licenses/by/4.0/).

1. Introduction

Condensation is a ubiquitous phenomenon in nature and is of interest in several technical applications, including water harvesting, seawater desalination, power generation, and so on [1–4]. The condensation heat transfer enhancement benefits to improving the energy utilization efficiency and saving energy in the industrial process. It is documented that condensation can be divided into filmwise condensation and dropwise condensation [5]. Filmwise condensation mainly occurs on the hydrophilic surface or under high subcooling conditions, where liquid film hinders the direct contact between the condensation surface and steam and hence leads to an increase in thermal resistance. Thus, rapid removal of the condensate and thinning of liquid film thickness can be utilized to enhance filmwise condensation heat transfer. Differing from filmwise condensation, dropwise condensation mainly occurs on the hydrophobic surface, which goes through the process of droplet nucleation, growth, coalescence, and departure. Owing to the rapid removal of droplets and constant emergence of nucleation sites, the heat transfer coefficient of dropwise condensation is one order of magnitude higher than that of filmwise condensation [6,7]. However, at high subcooling, the nucleation rate of droplets increases rapidly, and the occurrence of flooding increases the heat transfer resistance since the condensate cannot be shed in time. As a result, the dropwise condensation would transform into filmwise condensation, deteriorating the heat transfer performance [8,9]. In this context, it is urgent to develop

an efficient way to remove the condensate droplet on a cold wall and hence enhance dropwise condensation.

Condensate on the hydrophobic surface can shed rapidly, while the high energy barrier makes droplet nucleation difficult [10,11]. In recent years, researchers have developed a series of hybrid surfaces containing both hydrophilic and hydrophobic parts to make comprehensive use of both benefits of each surface [12–16]. For example, the liquid film on the hydrophilic area can suck and transport the droplets on the hydrophobic area quickly through striped hydrophilic modification on the hydrophobic surface [17–19], which reduces the droplet detachment diameter and accelerates the renewal frequency of droplets on the hydrophobic area. Although sacrificing part of the hydrophobic area with high heat transfer performance, the rapid condensate departure effect due to the liquid film transportation on the hydrophilic area will enhance the heat transfer on the rest hydrophobic area. In this way, a better comprehensive condensation heat transfer performance can be obtained. In the 1990s, Kumagai et al. [20] first explored the condensation heat transfer enhancement of the hybrid surface with the coexistence of dropwise and filmwise condensations. The surface was divided into finer patterns, such as horizontal or vertical stripes. However, in their works, the improvement of condensation heat transfer performance on the hybrid surface was limited, the heat flux of which was weaker than that of a full hydrophobic surface. This is because they failed to balance the benefits and losses of introducing the hydrophilic part into the hydrophobic surface, which needs further investigation. In 2015, Peng et al. [15] carried out a similar experimental study in pure steam conditions, mainly exploring the influence of the size of hydrophilic and hydrophobic stripe structures on condensation heat transfer performance. It is found that with the increase in the hydrophobic region width, the condensation heat transfer coefficient increased at first and then decreased, that is, there was an optimal hydrophobic region width. The heat flux of the optimal hybrid surface was 23% higher than that of complete dropwise condensation on the hydrophobic surface at subcooling 2 K. Recently, Wang et al. [21] carried out experimental research to investigate the heat transfer performances of tubes with hybrid hydrophilic–hydrophobic surfaces and functional fins. It is proven that the outer hydrophilic surface can decrease the resistance of droplet nucleation, while the inner hydrophobic surface can enhance the removal of droplets.

Compared with the above plane surfaces, the hydrophilic groove structure can help reduce the thickness of the liquid film on the top of the groove and transport the condensate at the bottom of the groove in time by surface tension, which reduces the thermal resistance of the liquid film in the groove. This contributes to the enhancement of filmwise condensation heat transfer performance [22–25]. Inspired by this, Ji et al. [26] enhanced condensation heat transfer by arranging the network of super-hydrophilic grooves on the hydrophobic stainless steel surface. In the work, super-hydrophilic grooves were used to replace the plain hydrophilic stripes on the traditional hybrid surface, and the transport performance of liquid film on the hydrophilic area was enhanced. Their results showed that the condensate on the hydrophobic region could be sucked away in time, reducing the droplet diameter and accelerating the departure of the condensate. The heat transfer coefficient was up to 3.4 times that of the plain hydrophobic surface. Differing from the super-hydrophilic–hydrophobic network hybrid surface proposed by Ji et al., Lo et al. [27] prepared a 3D hybrid surface with superhydrophobic ridge and hydrophilic microchannels. The droplets on the superhydrophobic ridge could move spontaneously into the hydrophilic groove, and the liquid bridges formed on the surface could also be removed through the groove, which increased the droplet detachment frequency on the hybrid surface at high subcooling. In their pure steam experiment, the heat transfer coefficient of the 3D hybrid surface was higher than that of the plane hydrophobic surface, and the maximum heat flux was about 3 times higher at subcooling 18 K.

Though most experiments and theoretical studies are based on pure steam, the condensation heat transfer performance and dynamics behaviors of droplets on the hybrid surface in humid air are also worth exploring. Because non-condensable gas is an important factor

affecting the condensation heat transfer performance, the condensation surface can show different condensation characteristics in pure steam and humid air.

Despite the superior condensation heat transfer performance of pure steam on hybrid surfaces [27], it is still unclear whether the hybrid surface improves the thermal performance of humid air condensation. In addition, the dynamic behaviors of the droplet on wettability-interval grooved surfaces during humid air condensation are not fully understood. To provide further insight into humid air condensation on hybrid surfaces, an experiment is conducted to investigate the condensation phase change process on wettability-interval grooved surfaces via a visualization system with high-speed CCD, to explore the droplet dynamic behaviors. In addition, the droplet dynamic behaviors and heat transfer performance of condensation on a wettability-interval grooved surface are compared with several corresponding surfaces, including the plain hydrophilic surface, plain hydrophobic surface, hydrophilic grooved surface, and hydrophobic grooved surface. The current visualization experiment identifies the thermal improvement of humid air condensation by using a wettability-interval micro-grooved surface.

2. Description of Experiment

2.1. Sample Preparation

A pure copper sheet with a size of 50 mm × 60 mm × 1 mm was used as the substrate in the experiment. The plain copper sheet was polished with 2000# sandpaper first, followed by ultrasonic cleaning in ethanol solution for 20 min to remove the impurities and oxides on the surface. For the hydrophilic surface, the cleaned copper sheet was immersed in the 30 wt% hydrogen peroxide aqueous solution for 2 h. After the reaction, a thin layer of CuO film was formed on the copper surface [28]. Finally, the hydrophilic copper surface was obtained after being cleaned with deionized water, purging, and drying with nitrogen.

As for the hydrophobic surface, the silane hydrophobic agent Soft99 (GLACO) was uniformly sprayed on the cleaned surface. After the solvent evaporated, the copper sheet was dried at 70 °C for 1 h to become hydrophobic. Using the above treatment, the plain hydrophobic surface was made.

To prepare the hydrophilic grooved surface, the microgrooves with 0.2 mm width, 0.2 mm depth, and 0.5 mm interval were fabricated through CNC machining based on the pure copper sheet.

To prepare the surface with wettability-interval microgrooves, the microgrooves with 0.2 mm width, 0.2 mm depth, and 0.5 mm interval were fabricated through CNC machining based on the hydrophobic copper sheet prepared in the previous step, and the preparation diagram is shown in Figure 1. Since the original copper substrate was hydrophilic, the machined channel was hydrophilic, and the ridge of the groove remained hydrophobic; thus, the copper surface with wettability-interval microgrooves was obtained and named the wettability-interval grooved surface.

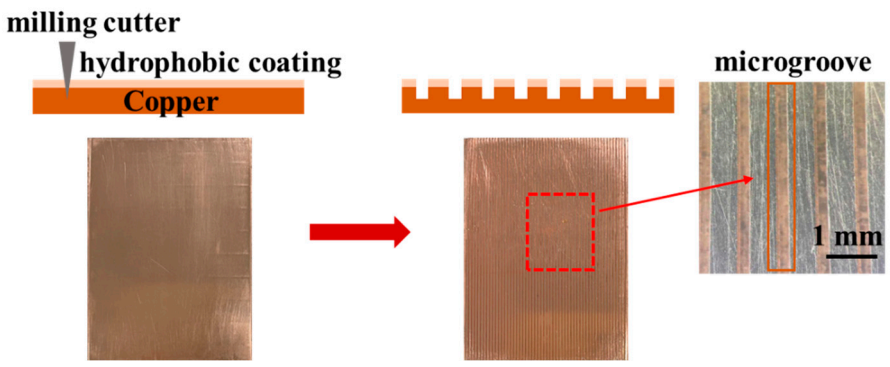


Figure 1. Diagram of preparation of surface with wettability-interval microgrooves. The part of the hydrophobic copper surface that has been grooved becomes hydrophilic and the remaining one is still hydrophobic.

2.2. Wettability

Surface wettability is an important factor affecting the condensate dynamic behaviors and heat transfer performance. The contact angles of various functional surfaces including hydrophilic pure copper grooved surface, hydrophobic grooved surface, and wettability-interval grooved surface were measured using the sessile drop method to characterize the surface wettability. Previous studies have suggested that the wettability on the surface with grooves shows anisotropic characteristics [29]. Therefore, the contact angles perpendicular and parallel to the groove direction were measured in this study and are shown in Figure 2. The results indicated that due to the extrusion of the groove, the spreading of droplets perpendicular to the groove direction was restricted so that the contact angle perpendicular to the groove direction was higher than that parallel to the groove direction. For example, on the hydrophilic pure copper grooved surface, the contact angles perpendicular and parallel to the groove direction were 90° and 80°, respectively. This is strongly associated with the hydrophilic and hydrophobic surface wetting modes. Droplets on hydrophilic surfaces exhibit an infiltrating Wenzel state [30], where the droplet edges are pinned to the surface and difficult to spread, so the external groove structure has a strong influence on the apparent contact angle. On the other hand, the droplets on hydrophobic surfaces show a suspended Cassie state, in which the droplets are constrained by the solid boundary in a relatively small way. The surface anisotropy on the wettability of the hydrophobic grooved surface was comparatively weak. The contact angles were perpendicular and parallel to the groove direction of the hydrophobic grooved surface were 142° and 138°, respectively. Related studies have demonstrated that the increase in hydrophobicity can weaken the wetting anisotropy of the surface with grooves [31]. On the wettability-interval grooved surface, the contact angle perpendicular to the groove direction was 125°, and that parallel to the groove direction was only 74°. This is due to the combined effect of the wettability difference between hydrophilic and hydrophobic surfaces and the geometric structure of grooves. The hydrophobic surface hinders the spreading of droplets so that droplets tend to spread on the hydrophilic surface; meanwhile, the ridge structure of the grooves acts as a restriction on the spreading of droplets in the vertical ridge direction, so that droplets are easily stretched out in the direction of the parallel grooves. Meanwhile, the ridge structure of the grooves acts as a restriction on the spreading of droplets in the vertical ridge direction, so that droplets are easily stretched out in the direction of the parallel grooves.

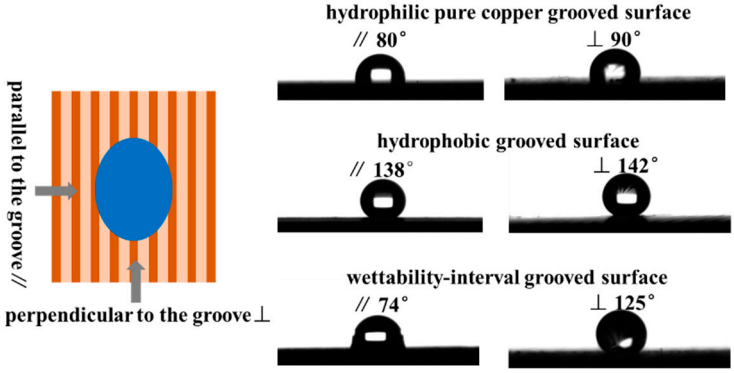


Figure 2. The wettability of samples. The // symbol in the figure indicates the apparent contact angle of this droplet stretching along the direction of the flat groove, whose viewing angle is shown to be in the vertical groove direction, while ⊥ is the opposite of it.

2.3. Test Section

The humid air condensation experimental platform was built to visually investigate the condensate dynamic behaviors and obtain the condensation heat flux on different functional surfaces. The experimental platform mainly consisted of a condensation chamber, a humidifier, a heat exchange plate, a water bath, and a high-speed CCD camera, as shown in Figure 3. In the condensation chamber, the surface to be tested was fixed to

the heat exchanger plate by screws in the vertical direction, on the top of which, four boreholes with the diameter of 0.5 mm and depth of 10 mm were drilled on the back of the sample to arrange thermocouples to measure the wall temperature of the surface. The distance between the condensation surface and the thermocouple was less than 1 mm. The water bath was connected to the inlet and outlet of the heat exchanger plate, and two thermocouples were arranged at the inlet and outlet of the heat exchanger plate separately to measure the temperature of the inlet and outlet water. The cooling water flow rate was measured by a turbine flow meter, and the wall temperature of the surface was controlled by adjusting the flow rate and temperature of the cooling water. The humidifier was used to increase the humidity in the chamber, and an exhaust fan was installed at the top of the chamber to enhance the air mixing. A temperature and humidity meter was arranged at 5 mm in front of the condensation surface to measure the humidity and temperature of the humid air. The heat exchange plate and pipes were wrapped with thermal insulation materials to reduce heat loss. The camera was used to record the condensation phenomenon on the surface.

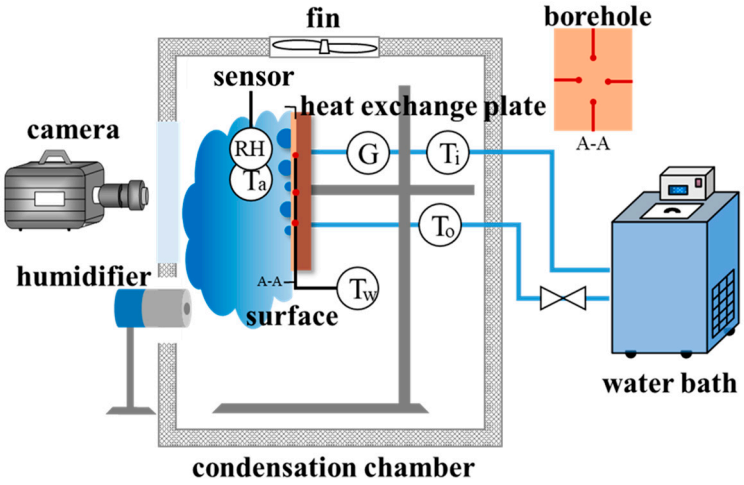


Figure 3. Schematic diagram of the experimental setup.

At standard atmospheric pressure, in a constant temperature room at 20 K, when the humidifier works stably, the relative humidity in front of the condensation surface can be maintained at 80 ± 3%. Before the start of the experiment, the flow rate and temperature of cooling water were adjusted to the set value. When the temperature of the wall, the inlet, and the outlet water of the heat exchange plate became stable, the humidifier was turned on, the temperature data were recorded, and the surface condensation phenomenon was recorded by a camera.

2.4. Data Reduction

The wall temperature was calculated using the average of the four thermocouples arranged on the back of the sample. The condensation heat flux can quantitatively describe the condensation heat transfer performance. In the experiment, the condensation heat flux was calculated by the water temperature difference between the inlet and outlet of the heat exchanger plate, that is:

$$q = \frac{C\dot{m}(T_{out} - T_{in})}{A} \quad (1)$$

where C was the specific heat capacity of water, m is the mass flow rate of cooling water, T_{in}, T_{out} was the temperature of inlet and outlet water of the heat exchange plate, and A was the condensation surface area.

The uncertainty of heat flux was analyzed using the error propagation theory, which can be expressed as follows:

$$\sigma_q = \sqrt{\left(\frac{\partial q}{\partial \mathrm{C}}\sigma_{\mathrm{C}}\right)^2 + \left(\frac{\partial q}{\partial \dot{m}}\sigma_{\dot{m}}\right)^2 + \left(\frac{\partial q}{\partial T_{\mathrm{in}}}\sigma_{T_{\mathrm{in}}}\right)^2 + \left(\frac{\partial q}{\partial T_{\mathrm{out}}}\sigma_{T_{\mathrm{out}}}\right)^2 + \left(\frac{\partial q}{\partial A}\sigma_A\right)^2} \quad (2)$$

where C was constant, the uncertainty of m was 1.04×10^{-4} kg/s according to the specification of the flow meter, the uncertainties of T_{in} and T_{out} were 0.2 K according to the resolution of T-type thermocouples, and the uncertainty of A was 2.5×10^{-9} m^2. The maximum uncertainty of heat flux was 4.7%.

3. Results and Discussion

3.1. Droplet Dynamic Behavior

3.1.1. Comparison of Droplet Dynamic Behaviors on Functional Surfaces

As indicated by the above contact angle measurement, the functional surfaces presented diverse wettability. To thoroughly understand the effect of surface wettability on the condensation characteristics in humid air, the condensate dynamic behaviors on different surfaces (plain hydrophilic surface, plain hydrophobic surface, hydrophilic grooved surface, hydrophobic grooved surface, and wettability-interval grooved surface) in humid air were compared and analyzed. The efforts are especially devoted to revealing the droplet growth and shedding characteristics.

Generally speaking, the filmwise condensation on the plain hydrophilic surface goes through four stages: nucleation, liquid film growth, merging, and shedding. On the plain hydrophilic surface, due to the large nucleation density and rate, the morphology of condensate was a thin liquid film. After a period of time, the small liquid film gradually merged into the large ones. The coalescence process is shown in Figure 4a. Because of the existence of high surface adhesion, the liquid film did not easily fall off and gradually merged into a larger liquid film covering the surface, and finally fell off due to gravity.

Droplet condensation occurs on the plain hydrophobic surface and usually goes through four stages: nucleation, droplet growth, coalescence, and shedding. The nucleation sites of the droplets were randomly distributed on the surface, and the small droplets grew into large droplets by either direct condensation or coalescence. The coalescence process is shown in Figure 4b. The droplet started to fall off when it reached a critical droplet radius where gravity could overcome the surface tension and adhesion force. The shedding droplets swept the downstream droplets and refreshed the condensation surface. Then, it was followed by new nucleation sites and repeated dropwise condensation. The droplets on the plain hydrophobic surface could slip off rapidly, and the liquid film covering the majority of the plain hydrophilic surface did not appear on plain hydrophobic surface.

On the hydrophilic grooved surface, liquid membranes appeared on the ridges and grooves during condensation. The liquid membranes gradually merged into a large liquid film covering the surface, which was similar to the plain hydrophilic surface, and the coalescence process is shown in Figure 4c. Finally, the flooded liquid film slipped off the surface due to gravity. The microgrooves were beneficial for the liquid film slip compared with the plain hydrophilic surface.

On the hydrophobic grooved surface, the nucleation process was different from that on a plain hydrophobic surface. The droplets nucleated preferentially at the edge of the groove due to the edge effect [32]. After growing to a certain volume, the droplets started to merge as shown in Figure 4d. The merged droplets on the ridge could stand on the top of the groove and did not collapse into the groove. The small droplets inside the grooves would also be absorbed by the large droplets on the ridge, so it was difficult to form the flowing liquid film in the grooves. Similar to the plain hydrophobic surface, when the droplets on the hydrophobic grooved surface reached the critical volume, they would fall off due to gravity and sweep the downstream droplets on the condensation surface; then, the new condensation process started again on the clean surface. On the surface with

uniform wettability, the sweeping behavior driven by gravity was the main way to remove the condensate.

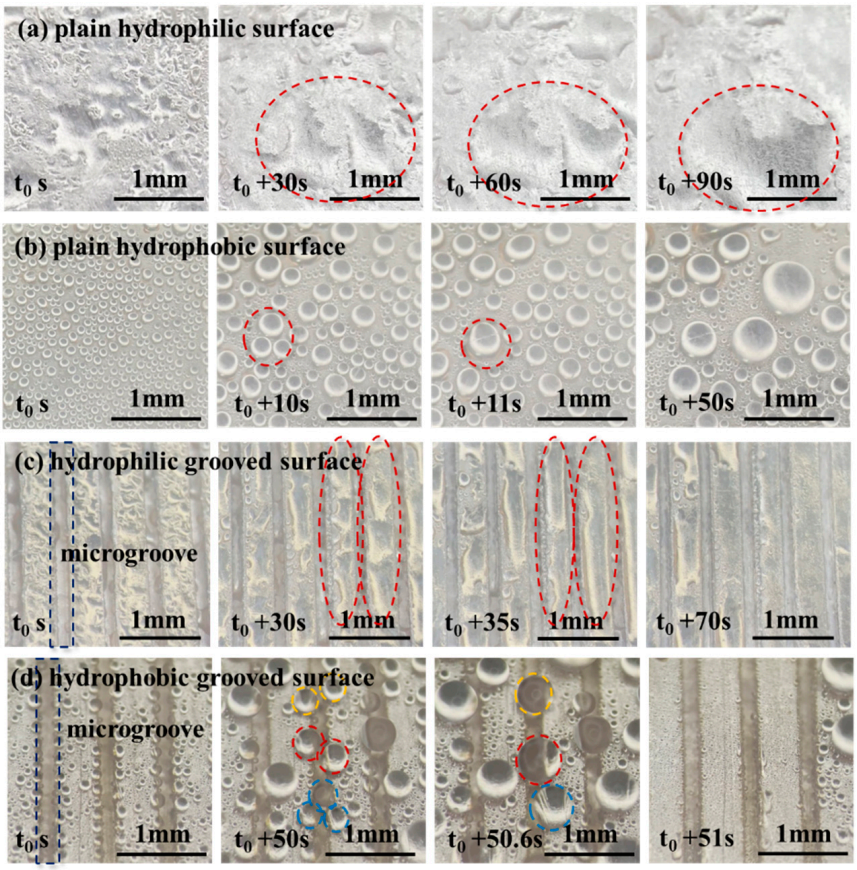


Figure 4. Condensate dynamic behaviors on the surfaces: (**a**) plain hydrophilic surface; (**b**) plain hydrophobic surface; (**c**) hydrophilic grooved surface; (**d**) hydrophobic grooved surface. The change process of the droplets or liquid is shown in the red circles.

On the wettability-interval grooved surface, the process of droplet nucleation was similar to that of a hydrophobic grooved surface, where nucleation sites preferentially occurred at the edge of the groove and were randomly distributed on the hydrophobic ridge, as shown in Figure 5a. Then, part of the droplets could reach the maximum droplet radius on the hydrophobic ridge, as shown in Figure 5b, while some droplets on the ridge near the edge of the grooves were merged or sucked into the hydrophilic groove without growing to the maximum droplet radius. In this context, the maximum radius of the droplet on the hydrophobic ridge depended on the wettability and width of the hydrophobic ridge. The diagram of the maximum droplet radius can be seen in Figure 5c. The droplets in the grooves could not be absorbed by droplets on the ridge, which was different from that on a hydrophobic grooved surface but gradually accumulated to liquid film, and the small droplets at the edge of the ridge would slide into the grooves, accelerating the formation of the liquid film in the hydrophilic grooves.

From the above analysis, it can be seen that the droplet shedding on the plain hydrophobic surface mainly depends on gravity, while on the wettability-interval grooved surface, spontaneous suction effect and directional drainage through grooves occurred under the action of wettability gradient and groove drainage, resulting in efficient removal of condensate. To reveal the enhancement of condensation performance on the wettability-interval grooved surface, the spontaneous suction effect and directional drainage behaviors via grooves will be discussed in detail.

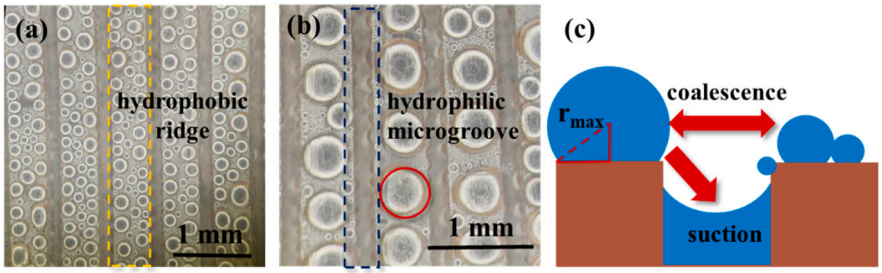


Figure 5. Droplet growth on the wettability-interval grooved surface: (**a**) dropwise condensation on the hydrophobic ridge; (**b**) droplets on the edge of the ridge and the maximum droplets on the ridge; (**c**) schematic diagram of suction effect and the maximum droplet radius.

3.1.2. Spontaneous Suction and Directional Drainage via Grooves

The spontaneous suction effect was a phenomenon in that when the droplets on the hydrophobic ridge were sucked by the liquid film in the hydrophilic groove, they could be sucked into the hydrophilic groove and merge with the liquid film spontaneously. This process, driven by the surface tension difference as shown in Figure 6a, increased the removal efficiency of droplets on the hydrophobic ridge. In addition, the spontaneous suction effect and the coalescence of droplets on the hydrophobic ridge would interact with each other, resulting in a chain effect. As shown in Figure 6b, when the droplets on the hydrophobic ridge were sucked into the groove, the volume of the liquid film in the groove would swell instantly, and then came into contact with the small droplets in the adjacent hydrophobic ridge, causing the coalescence of the small droplets and the liquid film. Finally, they all shed from the surface through the hydrophilic microgroove.

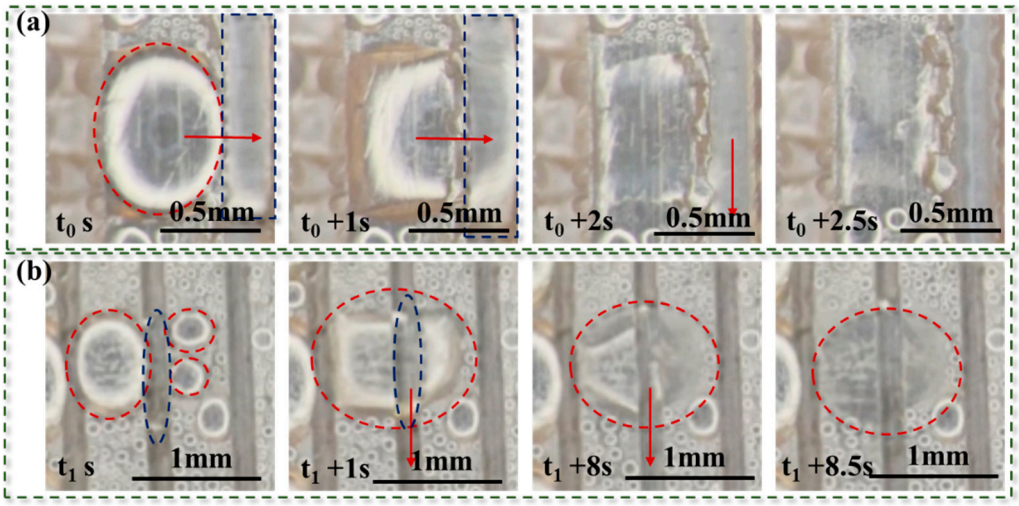


Figure 6. Spontaneous suction effect on the wettability-interval grooved surface. The blue circle indicates the liquid film movement, while the red circle shows the droplet and the red arrow indicates the direction of droplet movement: (**a**) spontaneous suction of signal droplet; (**b**) spontaneous suction effect induced droplets coalescence.

The formation of the liquid film in the groove was a prerequisite for the occurrence of the spontaneous suction phenomenon. If there was no liquid film forming in the groove, the spontaneous suction phenomenon hardly happened. If the droplets on the adjacent hydrophobic ridges could not be sucked into the groove and shed in time after coalescence, the formed large droplet would further grow into a liquid block across multiple hydrophobic regions. The formation of the liquid block would increase the thermal resistance of the surface, which would deteriorate condensation heat transfer performance. It should be pointed out that the effect of directional drainage through grooves could inhibit the

further growth of the liquid block into a flooded liquid film similar to that on a plain hydrophilic surface.

Directional drainage via grooves was a phenomenon that which after a liquid block covering multiple ridges formed on the surface, the condensate confined in the groove would flow downward along the groove due to gravity when it accumulated to a certain volume. Meanwhile, the liquid block outside the grooves continued to flow into the groove under the action of surface tension and the thickness of the liquid block gradually decreased until it completely shed through the groove. The schematic diagram is shown in Figure 7a. As a result, with the help of directional drainage, the critical volume required for the departure of the large liquid block was reduced. In other words, the wettability-interval grooved surface can effectively remove the condensate on the surface and inhibit the growth of the liquid block into the flooded liquid film. The removal of the liquid block from the surface by directional drainage is shown in Figure 7b, the whole process lasted about 2 s.

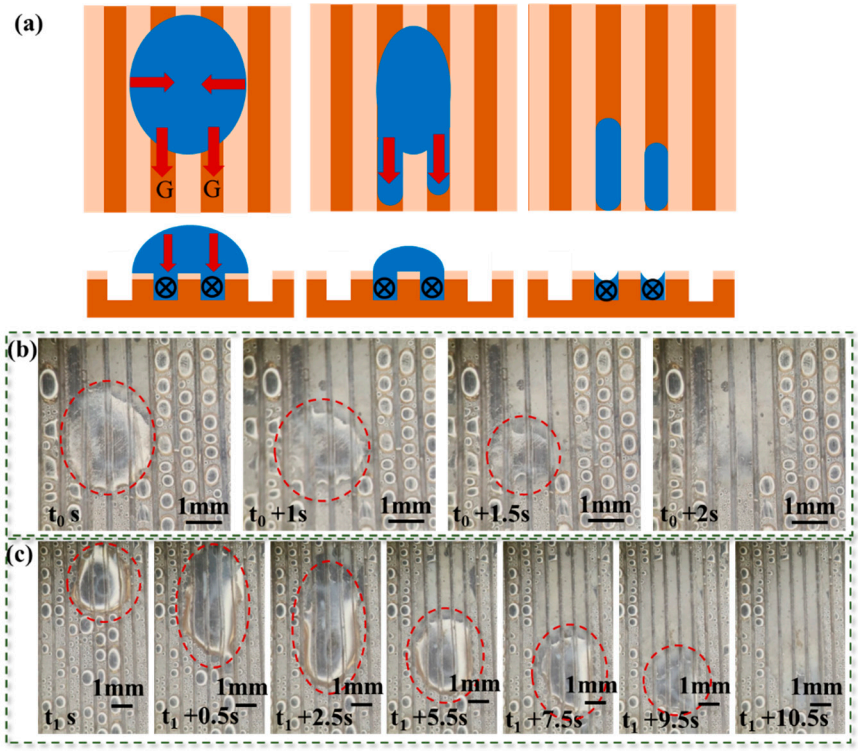


Figure 7. Directional drainage behaviors via microgrooves: (**a**) Schematic diagram of directional drainage behaviors; (**b**) Removal of the liquid block due to directional drainage behaviors; (**c**) Removal of the liquid block during downward sliding.

The directional drainage behaviors usually act on the condensate together with gravity. When the liquid block pinned to the surface grew to a certain volume through the coalescence of droplets and liquid film, the whole liquid block would slip downward due to gravity. In the process of shedding, the liquid block merged the downstream droplets, and the volume continued to increase. At the same time, the directional drainage behaviors could help reduce the volume of the large liquid block during the shedding process until the large liquid block vanishes and is transferred into the liquid film in the groove. As shown in Figure 7c, the whole process lasted about 10.5 s from the slippage initiation to the complete disappearance of the liquid block. It is noted that the downward flow of the liquid film in the groove could also result in a downstream spontaneous suction effect, which would further accelerate the removal of the condensate on the wettability-interval grooved surface.

The spontaneous suction effect and directional drainage behaviors via grooves were unique phenomena on the wettability-interval grooved surface. In humid air, the process

of shedding was usually a result of the coupling effects. A typical shedding process on the wettability-interval grooved surface was selected as an example, as shown in Figure 8.

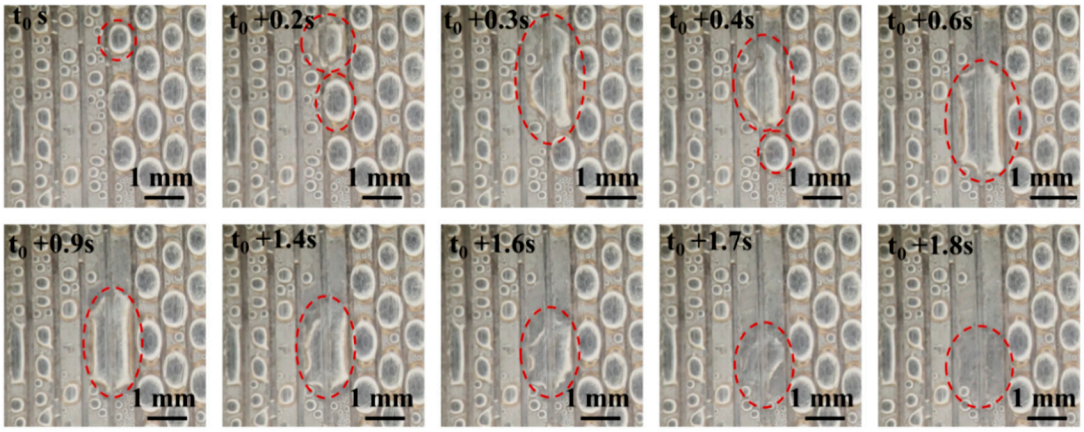


Figure 8. A typical shedding process on the wettability-interval grooved surface, including the progress of suck, film flow, and sweeping.

On the wettability-interval grooved surface, dropwise condensation occurred on the hydrophobic ridge, and the droplets reached the maximum droplet radius by either direct condensation or coalescence. When the droplet on the hydrophobic ridge came into contact with the liquid film in the hydrophilic groove, the droplet was sucked into the hydrophilic microgroove under the action of surface tension, which also induced the coalescence of droplets on the adjacent hydrophobic ridge. The coalescence process was rapid, and only lasted for 0.3 s. The coalescence accelerated the downward movement speed of the liquid film in the microgroove, and the other downstream droplets on the hydrophobic ridge were merged by the rapid downward liquid film in the microgroove, resulting in increased volume after the coalescence. After 1.8 s, the liquid block across the hydrophobic area gradually detached from the surface under the action of directional drainage via hydrophilic microgrooves, renewed surface for new dropwise condensation, and the downward liquid film in the groove would continue to suck the droplets on the downstream hydrophobic ridges. From the above analysis, it can be seen that the wettability-interval grooved surface showed efficient drainage performance under multiple actions.

3.2. Heat Transfer Performance

From the analysis of condensate dynamic behaviors on different functional surfaces, it can be seen that the dropwise condensation induced by the hydrophobic modification, especially the spontaneous suction effect and directional drainage behaviors induced by the wettability-interval microgrooves, are beneficial to the enhancement of the condensation heat transfer performance in the humid air. To quantitatively analyze the condensation heat transfer performance of different functional surfaces (including plain hydrophilic surface, plain hydrophobic surface, hydrophilic grooved surface, hydrophobic grooved surface, and wettability-interval grooved surface) in humid air, the corresponding condensation heat fluxes over time at subcooling of 12 K were compared in Figure 9.

As expected, surface wettability and microgrooves have a significant impact on the condensation heat flux in the humid air. As shown in Figure 9, when the condensation reached a steady state after a period of time, the heat flux of the hydrophobic surface was higher than that of the hydrophilic surface. The heat flux of the plain hydrophilic surface was the lowest, only 700 W/m^2, which was due to the large liquid film pinned on the plain hydrophilic surface. The increasing thermal resistance brought by large liquid film deteriorated condensation heat transfer performance. However, on the plain hydrophobic surface, the droplets could slide off rapidly from the surface owing to the low adhesion, resulting in lower thermal resistance. The heat flux of the plain hydrophobic surface

was 1030 W/m^2, much higher than that of the plain hydrophilic surface. In addition, for the surfaces with microgrooves, the heat flux of the hydrophobic grooved surface was 1110 W/m^2, which was higher than that of the hydrophilic grooved surface (768 W/m^2).

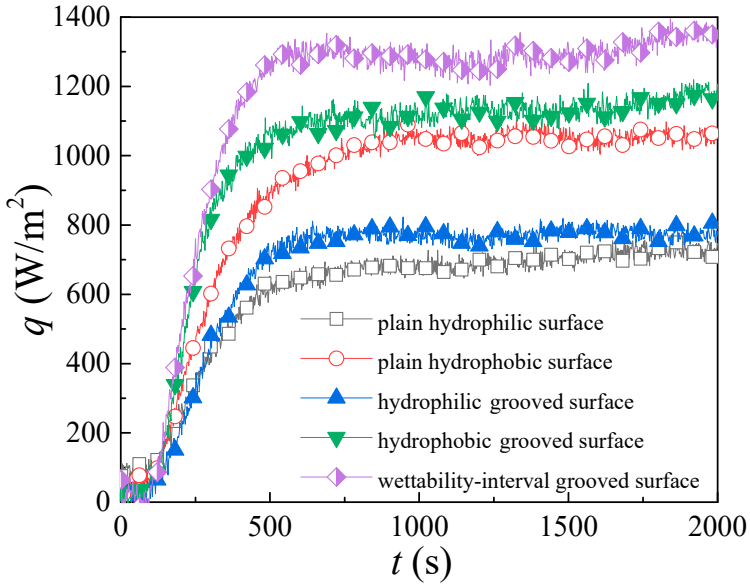


Figure 9. Comparison of condensation heat flux over time on different surfaces.

Even under the same surface wettability modification, the heat flux of the surface with microgrooves was higher than that of the plain surface in the humid air condensation. This was mainly since the microgroove structure increased the heat transfer area compared with the plain surface, and the microgroove structure could enhance the drag of condensate and accelerate the removal of the condensate on the surface. In addition, the heat flux of the plain hydrophobic surface was still higher than that of the hydrophilic grooved surface, so the surface wettability was the key factor affecting the condensation heat transfer performance. In some cases, surface wettability modification was more efficient than surface structure modification in enhancing condensation heat transfer performance.

Compared with the surfaces with uniform wettability, the wettability-interval grooved surface had the largest condensation heat flux. This was because large droplets, liquid film or liquid blocks pinned on the surface were easy to form on the surface with uniform wettability, which increased the heat transfer resistance of the condensation surface. However, the phenomenon of spontaneous suction and directional drainage through hydrophilic grooves could not only remove condensate quickly but also suppress the formation of the flooded liquid film. Therefore, the condensation heat flux on the wettability-interval grooved surface was the highest, which was 1280 W/m^2, about 1.8 times that of the plain hydrophilic surface (700 W/m^2), and 15% higher than that of the hydrophobic grooved surface (1110 W/m^2). This study demonstrated that the combined spontaneous suction and directional drainage phenomena were more efficient than the single gravity-driven sweeping mode in humid air with a large amount of non-condensable gas.

4. Conclusions

In summary, the wettability-interval grooved surface was found to have a stronger wettability anisotropic and unique condensed droplet dynamic behavior compared to other plain or grooved surfaces, which can effectively enhance humid air condensation heat transfer performance.

The presence of hydrophobic ridges perpendicular to the groove direction and hydrophilic grooves allows for the exclusion and easy spreading of droplets, respectively. Additionally, the coupling phenomena during condensation, such as spontaneous suction

and directional drainage via hydrophilic grooves, were only observed on the wettability-interval grooved surface and can quickly remove condensate while suppressing the formation of flooded liquid film. At subcooling of 12 K, the condensation heat flux on the wettability-interval grooved surface reaches 1280 W/m^2, which was 1.25 times higher than that of the plain hydrophobic surface, and 15% higher than that of the hydrophobic grooved surface, indicating exceptional heat transfer performance.

Author Contributions: Conceptualization, S.W. and Z.D.; Methodology, S.W. and Z.D.; Investigation, Z.D.; Data curation, S.G. and Z.X.; Writing—original draft, Z.D.; Writing—review & editing, S.R., S.G., Z.X. and S.W.; Visualization, S.G. and Z.X.; Supervision, S.R.; Project administration, S.R. All authors have read and agreed to the published version of the manuscript.

Funding: This work was supported by the National Natural Science Foundation of China (Grant No. 52306076), National Natural Science Foundation of China (Grant No. 52306230), and Natural Science Foundation of Jiangsu Province (No. BK20210239).

Data Availability Statement: No new data were created.

Conflicts of Interest: The authors declare no conflict of interest.

Nomenclature

Nomenclature	
q	heat flux/W·m^{-2}
C	specific heat capacity/J·kg^{-1}·K^{-1}
T	temperature/K
m	mass flow rate/kg·s^{-1}
A	surface area/m^2
Greek symbols	
σ	uncertainty
Subscripts	
in	inlet
out	outlet

References

1. Ahangar, S.B.; Lee, K.B.; Choi, C.K. Dropwise Condensation Mechanism on Smooth Hydrophilic Surfaces. *Appl. Sci.* **2021**, *11*, 9184. [CrossRef]
2. Ahangar, S.B.; Jeong, C.H.; Long, F.; Allen, J.S.; Lee, S.H.; Choi, C.K. The Effect of Adsorbed Volatile Organic Compounds on an Ultrathin Water Film Measurement. *Appl. Sci.* **2020**, *10*, 5981. [CrossRef]
3. Ma, X.H.; Wang, B.X.; Xu, D.Q.; Lin, J.F. Filmwise condensation heat transfer enhancement with dropwise and filmwise coexisting condensation surfaces. *Chin. J. Chem. Eng.* **1998**, *6*, 95–102.
4. Chen, Y.P.; Wu, R.; Shi, M.H.; Peterson, G.P. Visualization study of steam condensation in triangular microchannels. *Int. J. Heat Mass Transfer.* **2009**, *52*, 5122–5129. [CrossRef]
5. Chen, Y.P.; Shi, M.H.; Cheng, P.; Peterson, G.P. Condensation in microchannels. *Nanoscale Microscale Thermophys. Eng.* **2008**, *12*, 117–143. [CrossRef]
6. Boreyko, J.B.; Chen, C.H. Self-Propelled Dropwise Condensate on Superhydrophobic Surfaces. *Phys. Rev. Lett.* **2009**, *103*, 184501. [CrossRef]
7. Chen, C.H.; Cai, Q.; Tsai, C.; Chen, C.L.; Xiong, G.; Yu, Y.; Ren, Z. Dropwise condensation on superhydrophobic surfaces with two-tier roughness. *Appl. Phys. Lett.* **2007**, *90*, 173108. [CrossRef]
8. Cai, S.Q.; Bhunia, A.J. Superhydrophobic Condensation Enhanced by Conical Hierarchical Structures. *Phys. Chem. C* **2017**, *121*, 10047–10052. [CrossRef]
9. Wang, S.; Liu, M.; Feng, Y.; Bu, Y.; Huynh, S.H.; Ng, T.W.; Gu, F.; Yu, A. Bioinspired hierarchical copper oxide surfaces for rapid dropwise condensation. *J. Mater. Chem. A* **2017**, *5*, 21422–21428. [CrossRef]
10. Chen, X.; Wu, J.; Ma, R.; Hua, M.; Koratkar, N.; Yao, S. Nanograssed Micropyramidal Architectures for Continuous Dropwise Condensation. *Adv. Funct. Mater.* **2011**, *21*, 4617–4623. [CrossRef]
11. Wu, J.F.; Shi, M.H.; Chen, Y.P. Visualization study of steam condensation in wide rectangular silicon microchannels. *Int. J. Therm. Sci.* **2010**, *49*, 922–930. [CrossRef]
12. Tokunaga, A.; Tsuruta, T. Enhancement of condensation heat transfer on a microstructured surface with wettability gradient. *Int. J. Heat Mass Transfer.* **2020**, *156*, 119839. [CrossRef]

13. Egab, K.; Alwazzan, M.; Peng, B.; Oudah, S.K.; Guo, Z.; Dai, X.; Khan, J.; Li, C. Enhancing filmwise and dropwise condensation using a hybrid wettability contrast mechanism: Circular patterns. *Int. J. Heat Mass Transfer.* **2020**, *154*, 119640. [CrossRef]
14. Yang, K.S.; Lin, K.H.; Tu, C.W.; He, Y.Z.; Wang, C.C. Experimental investigation of moist air condensation on hydrophilic, hydrophobic, superhydrophilic, and hybrid hydrophobic-hydrophilic surfaces. *Int. J. Heat Mass Transfer.* **2017**, *115*, 1032–1041. [CrossRef]
15. Peng, B.; Ma, X.; Lan, Z.; Xu, W.; Wen, R. Experimental investigation on steam condensation heat transfer enhancement with vertically patterned hydrophobic-hydrophilic hybrid surfaces. *Int. J. Heat Mass Transfer.* **2015**, *83*, 27–38. [CrossRef]
16. Hu, H.W.; Tang, G.H.; Niu, D. Experimental investigation of condensation heat transfer on hybrid wettability finned tube with large amount of noncondensable gas. *Int. J. Heat Mass Transfer.* **2015**, *85*, 513–523. [CrossRef]
17. Oestreich, J.; Geld, C.; Oliveira, J.; Silva, A. Experimental condensation study of vertical superhydrophobic surfaces assisted by hydrophilic constructal-like patterns. *Int. J. Therm. Sci.* **2019**, *135*, 319–330. [CrossRef]
18. Lee, J.; Lee, S.; Lee, J. Improved humid air condensation heat transfer through promoting condensate drainage on vertically stripe patterned bi-philic surfaces. *Int. J. Heat Mass Transfer.* **2020**, *160*, 120206. [CrossRef]
19. Alwazzan, M.; Egab, K.; Peng, B.; Khan, J. Condensation on hybrid-patterned copper tubes (I): Characterization of condensation heat transfer. *Int. J. Heat Mass Transfer.* **2017**, *112*, 991–1004. [CrossRef]
20. Kumagai, S.; Tanaka, S.; Katsuda, H.; Shimada, R. On the Enhancement of Filmwise Condensation Heat Transfer by Means of the Coexistence with Dropwise Condensation Sections. *Exp. Heat Transf.* **1991**, *4*, 71–82. [CrossRef]
21. Wan, Z.; Hu, X.; Wang, X.; He, Z. Experimental study on the bolling/condensation heattransfer performance of a finned tube wih a hydrophllic/hydrophobic surface. *Appl. Therm. Eng.* **2023**, *229*, 120494. [CrossRef]
22. Park, I.S.; Choi, D.H. Heat- and mass-transfer analysis for the condensing film flow along a vertical grooved tube. *Int. J. Heat Mass Transf.* **2001**, *44*, 4277–4285. [CrossRef]
23. Sommers, A.D.; Jacobi, A.M. Wetting phenomena on micro-grooved aluminum surfaces and modeling of the critical droplet size. *J. Colloid Interface Sci.* **2008**, *328*, 402–411. [CrossRef] [PubMed]
24. Rahman, M.A.; Jacobi, A.M. Wetting behavior and drainage of water droplets on microgrooved brass surfaces. *Langmuir.* **2012**, *28*, 13441–13451. [CrossRef]
25. Wu, J.F.; Chen, Y.P.; Shi, M.H.; Fu, P.P.; Peterson, G.P. Three-Dimensional Numerical Simulation for Annular Condensation in Rectangular Microchannels. *Nanoscale Microscale Thermophys. Eng.* **2009**, *13*, 13–29. [CrossRef]
26. Ji, X.; Zhou, D.; Dai, C.; Xu, J. Dropwise condensation heat transfer on superhydrophilic-hydrophobic network hybrid surface. *Int. J. Heat Mass Transfer.* **2019**, *132*, 52–67. [CrossRef]
27. Lo, C.W.; Chu, Y.C.; Yen, M.H.; Lu, M.C. Enhancing Condensation Heat Transfer on Three-Dimensional Hybrid Surfaces. *Joule* **2019**, *3*, 2806–2823. [CrossRef]
28. Vemuri, S.; Kim, K.J.; Wood, B.D. Long term testing for dropwise condensation using self-assembled monolayer coatings of n-octadecyl mercaptan. *Appl. Therm. Eng.* **2006**, *26*, 421–429. [CrossRef]
29. Drelich, J.; Wilbur, J.L.; Miller, J.D.; Whitesides, G.M. Contact Angles for Liquid Drops at a Model Heterogeneous Surface Consisting of Alternating and Parallel Hydrophobic/Hydrophilic Strips. *Langmuir* **1996**, *12*, 1913–1922. [CrossRef]
30. Mohammadpour, L.; Moghadasi, H.; Saffari, H. Computational fluid dynamics investigation of dropwise condensation heat transfer through a single droplet on Wenzel structures. *Int. Commun. Heat Mass Transf.* **2023**, *145 Pt B*, 106853. [CrossRef]
31. Peng, Q.; Jia, L.; Ding, Y.; Dang, C.; Yin, L.; Yan, X. Influence of groove orientation on dropwise condensation on hydrophobic and hierarchical superhydrophobic surfaces with microgroove arrays. *Int. Commun. Heat Mass Transf.* **2020**, *112*, 104492. [CrossRef]
32. Medici, M.G.; Mongruel, A.; Royon, L.; Beysens, D. Edge effects on water droplet condensation. *Phys. Rev. E* **2014**, *90*, 062403. [CrossRef] [PubMed]

Disclaimer/Publisher's Note: The statements, opinions and data contained in all publications are solely those of the individual author(s) and contributor(s) and not of MDPI and/or the editor(s). MDPI and/or the editor(s) disclaim responsibility for any injury to people or property resulting from any ideas, methods, instructions or products referred to in the content.